ORIGINAL PAPER

Preparation of polyaniline–tin dioxide composites and their application in methanol electro-oxidation

Haili Pang · Changting Huang · Jinhua Chen · Bo Liu · Yafei Kuang · Xiaohua Zhang

Abstract Polyaniline–tin dioxide (PANI-SnO$_2$) composites were prepared by chemical polymerization method, and characterized by scanning electron microscopy, transmission electron microscopy, Fourier transform infrared spectroscopy, and X-ray diffraction. Due to the good stability in diluted acidic solution, PANI-SnO$_2$ composites were selected as the catalyst support and second catalyst for methanol electro-oxidation. The electrocatalytic properties of the PANI-SnO$_2$ supported Pt catalyst (Pt/PANI-SnO$_2$) for methanol oxidation have been investigated by cyclic voltammetry, chronoamperometry, and chronopotentiometry. Under the same loading mass of Pt, the Pt/PANI-SnO$_2$ catalyst shows higher electrocatalytic activity towards methanol electro-oxidation than Pt/SnO$_2$ catalyst.

Keywords PANI-SnO$_2$ composites ·
Pt/PANI-SnO$_2$ catalyst · Electrocatalytic activity ·
Methanol electro-oxidation · Electrochemical properties

Introduction

In recent years, great attention has been paid to the electro-oxidation of small organic molecules mainly due to their potential application as fuel in the anode reaction of fuel cells. Therefore, regarding the electro-oxidation of methanol and the construction of direct methanol fuel cell (DMFC), intense research efforts have been made in the last two decades [1, 2]. Although DMFC is proposed

H. Pang · C. Huang · J. Chen (✉) · B. Liu · Y. Kuang · X. Zhang
State Key Laboratory of Chemo/Biosensing and Chemometrics,
College of Chemistry and Chemical Engineering,
Hunan University,
Changsha 410082, People's Republic of China
e-mail: chenjinhua@hnu.cn

to be a kind of promising power source due to its high energy-conversion efficiency, some obstacles, such as low methanol oxidation kinetics and methanol permeation across the proton exchange membrane, still exist for its commercialization. It is well known that platinum is considered as the best single metal catalyst for methanol oxidation, but the poisoning of platinum catalyst by intermediates such as CO$_{ads}$ is the main reason for the low kinetics of methanol electro-oxidation [3, 4]. Nowadays, it was reported that the introduction of oxides (such as WO$_3$ [5, 6], CeO$_2$ [7, 8], RuO$_2$ [9]) is efficient to improve the catalytic activity of Pt for the oxidation of methanol.

SnO$_2$, one of the most widely used metal oxide catalysts for CO oxidation [10–12], is quite stable in diluted acidic solution. Because of its unique physicochemical properties, SnO$_2$ has also been used as the catalyst or catalyst support for oxidation of various kinds of hydrocarbons [13]. Preliminary studies indicated that the presence of tin oxides in Pt catalyst led to higher current densities in acid solution for the electro-oxidation of methanol in comparison with the case of pure platinum catalyst [14]. They deduced that SnO$_2$ in the vicinity of Pt nanoparticles could offer oxygen species conveniently to remove the CO-like species and free Pt active sites. However, for a good electrocatalyst, except CO-tolerance ability, electronic conductivity is also an important aspect, especially in real fuel cells. Therefore, as a semi-conductive oxide, the electronic conductivity of SnO$_2$ particles still needs to be improved if it is used as the catalyst in DMFC.

It is well documented that the addition of conductive additives can enhance the electronic conduction between active materials during redox reactions [15–17]. The electronic conductivity of the conducting polymers, which is as high as the metallic conductivity, attracts great interest

from an electrochemical viewpoint. Some conducting polymers have been studied for their catalytic behavior towards electrochemical reactions [18, 19]. Among this type of polymers, polyaniline (PANI) is one of the most studied conducting polymers because of its good electrical conductivity, environmental stability, and relative easy synthesis [20]. Besides, it was reported that PANI could be a good conducting matrix for the dispersion of Pt catalyst particles in methanol electro-oxidation [19, 21]. However, to the best of our knowledge, there are no works focusing on the application of PANI-SnO_2 composites in fuel cells, although the PANI-SnO_2 composites have already been studied as the optical, gas sensing, and supercapacitive materials [22–24]. Therefore, the PANI-SnO_2 composites were prepared in this paper and used as the catalyst support and the second catalyst for methanol oxidation. The electrocatalytic properties of the PANI-SnO_2 composites supported Pt catalyst (Pt/PANI-SnO_2) for methanol elelctro-oxidation have been investigated by cyclic voltammetry (CV), chronoamperometry (CA), and chronopotentiometry (CP).

Experimental section

Preparation and characterization of the PANI-SnO_2 composites

SnO_2 nanoparticles were synthesized by sol–gel method according to the same procedure mentioned in our previous work [25]. Two grams of $SnCl_2\cdot2H_2O$ was dissolved in 120 mL ethanol and a suitable amount of 0.5 M Na_2CO_3 aqueous solution was added drop-wise under ultrasonic stirring to obtain a sol, then aged overnight. After filtration and washed with double-distilled water for several times, the resulted deposit was dried at 80 °C for 4 h, then grounded and calcinated at 450 °C in air for 3 h to obtain SnO_2 nanoparticles.

Aniline monomer were added into 1 M HCl solution and ultrasonically treated for 30 min, then a specific amount of SnO_2 powder (the molar ratio of aniline to SnO_2 was 1:3) was added. The mixture was stirred and ultrasonically treated for 1 h each, then a definite amount of ammonium peroxydisulfate (APS) dissolved in 1 M HCl solution (the molar ratio of aniline to APS was 1:1) was added drop-wise within 1 h and the reaction time was 5 h under vigorous stirring. The resulted green dispersion was centrifuged and washed by 0.2 M HCl solution and double-distilled water for several times. Then washed by acetone and the resulted deposit was dried at 60 °C in vacuum for 4 h to obtain the PANI-SnO_2 composites.

The surface morphology of the PANI-SnO_2 composites was analyzed by scanning electron microscopy (SEM,

JSM 5600 LV, 30 kV) and transmission electron microscopy (TEM, JEM-3010). The crystal structure was examined by X-ray diffraction (XRD, D/MAX-RA). Fourier transform infrared (FTIR) spectrum was recorded on a NICOLET 6700 spectrophotometer using KBr pellets.

Preparation, characterization, and electrochemical measurements of the Pt/PANI-SnO_2 catalyst

PANI-SnO_2 powder, 2.0 mg, was dispersed in 4 mL of double-distilled water and then mixed with 90 μL of 38.6 mM H_2PtCl_6 aqueous solution under ultrasonic stirring. The excess fresh $NaBH_4$ solution was added drop-wise into the mixture and the solution color was changed from yellow to black. This suggested that the Pt/PANI-SnO_2 hybrid catalyst was formed. A definite volume of the catalyst ink was then transferred onto the surface of the glassy carbon (GC) electrode by a micro-syringe. After drying in air, the electrode was coated with 5 μL of 0.05 wt.% Nafion ethanol solution.

For comparison, the Pt/SnO_2 catalyst was also prepared and transferred onto the surface of the GC electrode according to the same procedure mentioned above.

The morphology of the Pt/PANI-SnO_2 catalyst was characterized by transmission electron microscopy (TEM, JEM-3010).

The electrochemical properties of the Pt/PANI-SnO_2/GC and Pt/SnO_2/GC electrodes were investigated in 0.5 M H_2SO_4+1.0 M CH_3OH aqueous solution by electrochemical methods, those were carried out on a CHI 660A electrochemical working station (Chenhua Instrument Company of Shanghai, China) at 25 °C. A standard three-electrode cell was employed with platinum wire as the counter electrode and saturated calomel electrode as the reference electrode. As the working electrode, the GC electrodes with an exposure area of 0.2 cm^2 were used to support catalysts.

Results and discussion

Characterization of the PANI-SnO_2 composites and the Pt/PANI-SnO_2 catalyst

The micrographs of the PANI-SnO_2 composites have been investigated by SEM and TEM, and the corresponding results are shown in Fig. 1. From Fig. 1, we can estimate the particle size of the PANI-SnO_2 composites to be about 17 nm. Besides it can be seen that some of the spherical particles with clear boundaries are bare SnO_2, and other spherical particles with blurry boundaries are SnO_2 enwrapped by PANI.

Fig. 1 SEM (**a**) and TEM (**b**) images of the PANI-SnO$_2$ composites
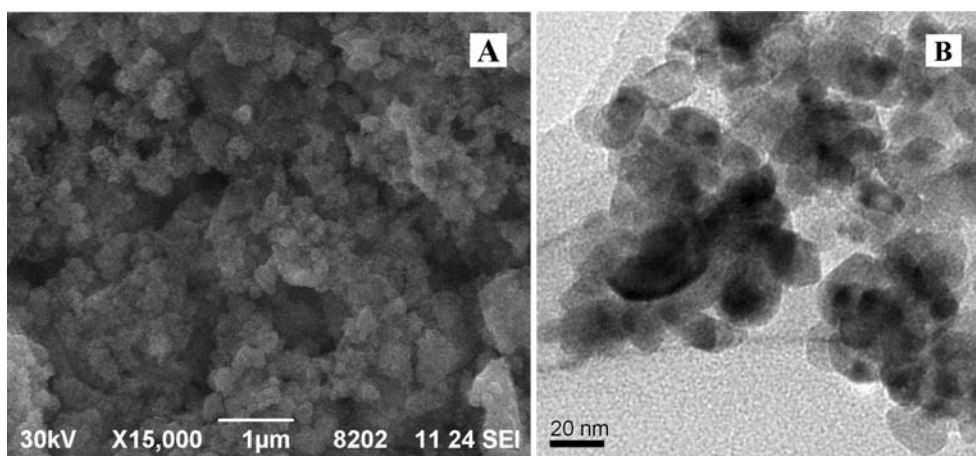
The structural information about the PANI-SnO$_2$ composites has been investigated by XRD and the corresponding results are shown in Fig. 2. For comparison, the XRD patterns of pure SnO$_2$ and PANI are also presented in Fig. 2. The diffraction patterns were collected using a fixed Cu Kα radiation ($\lambda = 1.54056$ Å) at 50 kV, 100 mA. It can be seen that the PANI-SnO$_2$ composites have the same profiles as pure SnO$_2$, indicating that the crystal structure of SnO$_2$ is not modified by PANI. However, the diffraction peaks of pure PANI at around 15.5°, 20.4°, and 25.2° were not observed in the XRD pattern of the PANI-SnO$_2$ composites, indicating that SnO$_2$ nanoparticles hamper the crystallization of PANI. This is consistent with that reported by Wang [26] and He [27].

Figure 3 shows the FTIR spectra of the PANI-SnO$_2$ composites and pure PANI in the range of 400–2,000 cm^{-1}. PANI exhibits characteristic bands at 1,580, 1,496, 1,300, 1,142, and 793 cm^{-1} [22, 28]. The bands at 1,580 and 1,496 cm^{-1} are attributed to C=N and C=C stretching bond in benzenoid ring; The peaks at 1,300 and 1,142 cm^{-1} are assigned to C–N stretching mode of benzenoid ring, and the peak at 1,142 cm^{-1} is the characteristic of the conducting

protonated form of PANI; the bond at 793 cm^{-1} originates out of C–H plane bending vibration. These characteristic peaks can also be observed in the FTIR spectrum of PANI-SnO$_2$ composites. And in the spectrum of PANI-SnO$_2$ composites, a new strong peak around 645 cm^{-1}, which corresponds to the stretching bond of Sn–O mode of SnO$_2$, could be observed.

The TEM images of the Pt/PANI-SnO$_2$ (image A) and Pt/SnO$_2$ (image B) catalysts are shown in Fig. 4. From Fig. 4a, it can be seen that Pt nanoparticles are dispersed uniformly on the PANI-SnO$_2$ composites and with the average diameters of about 3.2 nm. In Fig. 4b, we can obtain the size of Pt particles on SnO$_2$ to be about 4.3 nm. The size distribution of Pt nanoparticles for the Pt/PANI-SnO$_2$ and Pt/SnO$_2$ catalysts are also presented in Fig. 4c and d, respectively. It is obvious that the size of Pt nanoparticles for the Pt/PANI-SnO$_2$ catalysts is smaller than that for the Pt/SnO$_2$ catalysts.

Electrochemical properties of the Pt/PANI-SnO$_2$ catalyst

It is well known that the electrochemical surface area (ESA) is one of the important parameters for electro-
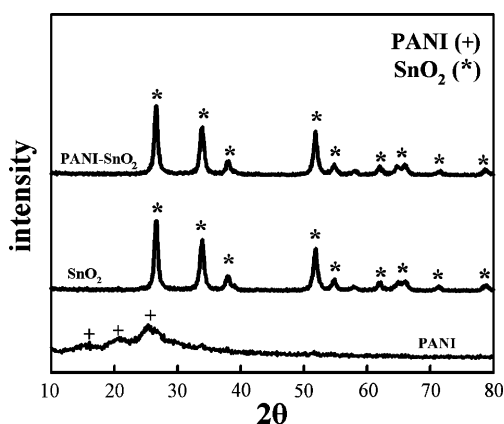

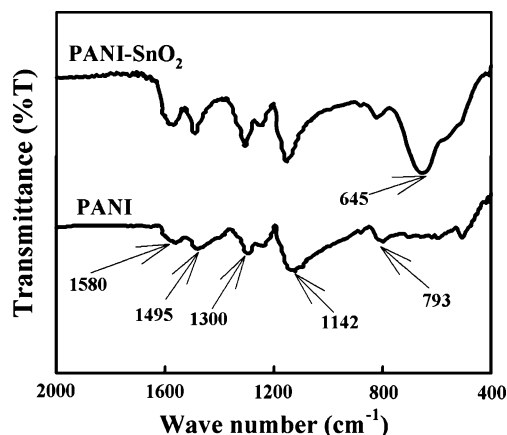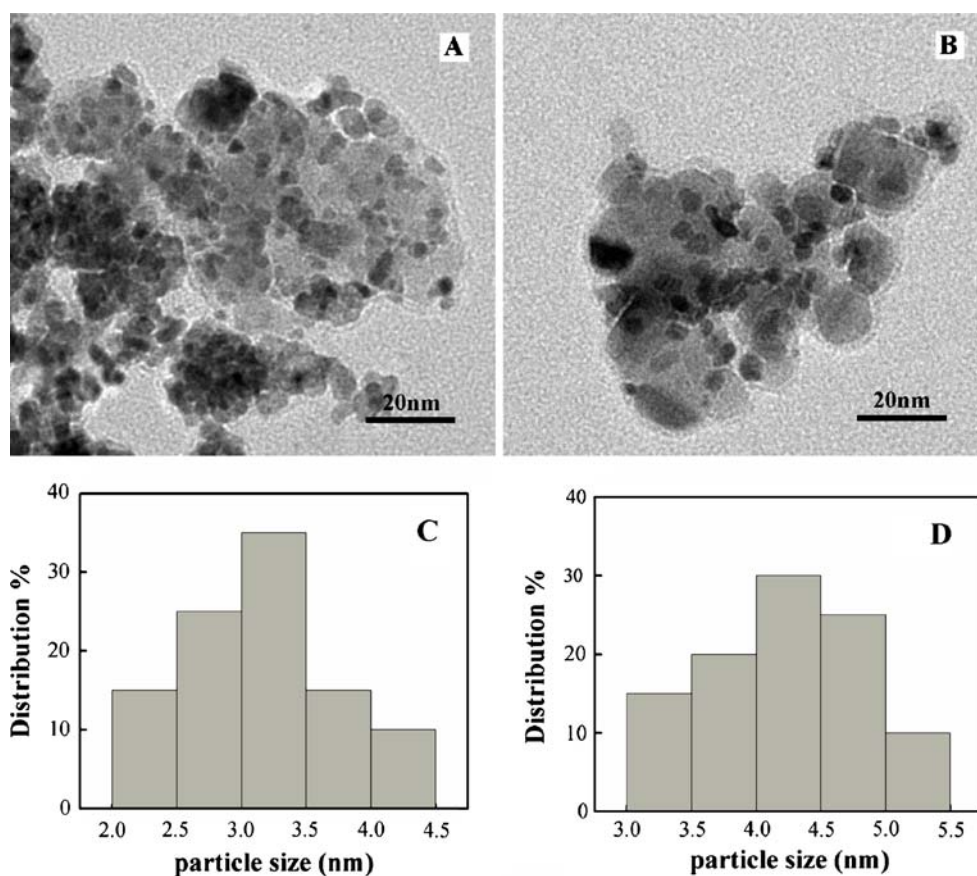Fig. 2 XRD patterns of the PANI-SnO$_2$ composites, pure SnO$_2$, and PANI

Fig. 3 FTIR spectra of the PANI-SnO$_2$ composites and pure PANI

Fig. 4 TEM images of the Pt/PANI-SnO$_2$ (**a**) and Pt/SnO$_2$ (**b**) catalysts; and histograms representing the size distribution of Pt nanoparticles in Pt/PANI-SnO$_2$ (**c**) and Pt/SnO$_2$ (**d**) catalysts

catalysts. To obtain the ESA values of the catalysts, cyclic voltammograms of the Pt/PANI-SnO$_2$/GC and Pt/SnO$_2$/GC electrodes have been recorded in 0.5 M H$_2$SO$_4$ aqueous solution and the results are presented in Fig. 5. In Fig. 5, the atomic hydrogen adsorption/desorption peaks were observed at around −0.25–0.05 V. According to Fig. 5, the ESA values of the Pt/PANI-SnO$_2$ and Pt/SnO$_2$ catalysts can be estimated using the following equation [29]:

$$ESA = Q_H/0.21 \times [Pt] \qquad (1)$$

where Q_H (mC cm^{-2}) represents the charge for the atomic hydrogen desorption, [Pt] is the Pt loading (mg cm^{-2}) on the electrode and 0.21 represents the charge required to oxidize a monolayer of the atomic hydrogen on bright Pt. According to Fig. 5 and Eq. 1, the ESA values of the Pt/PANI-SnO$_2$ and Pt/SnO$_2$ catalysts can be calculated and are about 48.6 m^2 g^{-1} and 23.8 m^2 g^{-1}, respectively. It is obvious that the Pt catalyst deposited on the PANI-SnO$_2$ composites shows the larger ESA value than that on the SnO$_2$. The reasons may be that PANI on the surface of SnO$_2$ particles is beneficial to the dispersion of Pt nanoparticles [30] and smaller particle size of Pt on the PANI-SnO$_2$ composites (Fig. 4).

The electrocatalytic properties of the Pt/PANI-SnO$_2$ catalyst for methanol oxidation have been investigated by CV in 0.5 M H$_2$SO$_4$+1.0 M CH$_3$OH aqueous solution and the corresponding results are shown in Fig. 6 (curve I). For comparison, the cyclic voltammogram of the Pt/SnO$_2$ catalyst (curve II) is also presented. As seen from Fig. 6, for both Pt/PANI-SnO$_2$ and Pt/SnO$_2$ catalysts, two oxidation peaks which are related to the oxidation of methanol (peak a) and the corresponding intermediates (peak b) produced during the methanol oxidation can be observed. The peak current (peak a) of methanol oxidation on the Pt/
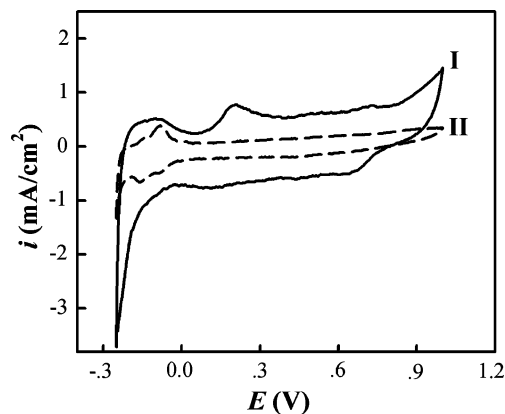

Fig. 5 Cyclic voltammograms of the Pt/PANI-SnO$_2$/GC (curve *I*) and Pt/SnO$_2$/GC (curve *II*) electrodes at 50 mV s^{-1} in 0.5 M H$_2$SO$_4$ aqueous solution. The loading mass of Pt, 4 μg
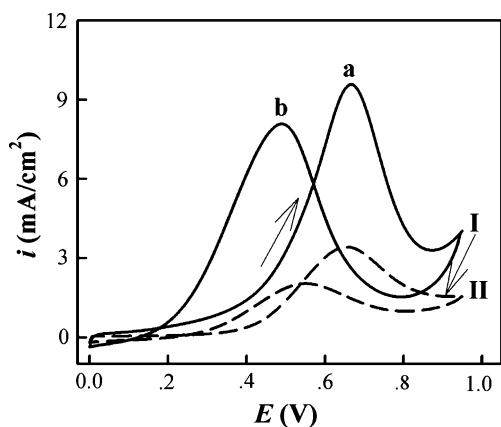
Fig. 6 Cyclic voltammograms of the Pt/PANI-SnO$_2$/GC (curve *I*) and Pt/SnO$_2$/GC (curve *II*) electrodes at 50 mV s^{-1} in 0.5 M H$_2$SO$_4$+ 1.0 M CH$_3$OH aqueous solution. The loading mass of Pt, 8 μg

PANI-SnO$_2$/GC electrode is 9.5 mA cm^{-2}, which is about 2.6 times as high as that on the Pt/SnO$_2$/GC electrode (3.6 mA cm^{-2}) under the same mass loading of Pt and experimental conditions. This implies that the electro-catalytic activity of the Pt/PANI-SnO$_2$/GC electrode is much higher than that of the Pt/SnO$_2$/GC electrode. The CV results can also be confirmed further from the results of CA shown in Fig. 7. From Fig. 7, it can be observed that during the whole time, the current density of methanol oxidation on the Pt/PANI-SnO$_2$/GC electrode (curve I) is higher than that on the Pt/SnO$_2$/GC electrode (curve II), which is consistent with the results from CV. This may be explained as follows: the introduction of PANI leads to smaller particle size of Pt and higher ESA, resulting in better electrocatalytic activity of the Pt/PANI-SnO$_2$/GC catalyst.

On the other hand, chronopotentiometry is a useful approach to study the anti-poisoning abilities of catalysts
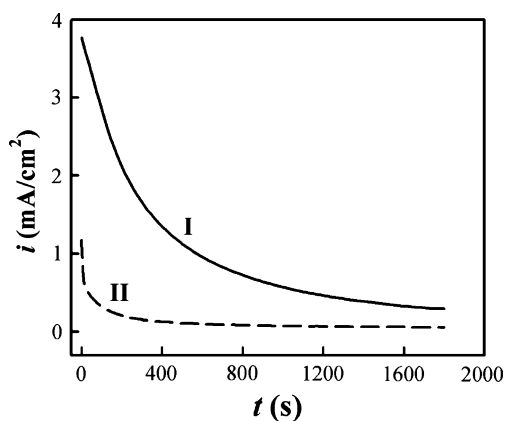
for alcohol oxidation [31]. The Pt/PANI-SnO$_2$ catalyst was characterized by CP and compared with the Pt/SnO$_2$ catalyst. From Fig. 8, it can be observed on both Pt/PANI-SnO$_2$/GC and Pt/SnO$_2$/GC electrodes that the electrode potential increases gradually for several seconds and then jumps to a higher potential. However, the Pt/PANI-SnO$_2$/GC electrode (curve I) has sustained a much longer time (about 520 s) before the potential jump than the Pt/SnO$_2$/GC electrode (curve II, about 150 s). This implies that the Pt/PANI-SnO$_2$ catalyst has better anti-poisoning ability than the Pt/SnO$_2$ catalyst. The improved anti-poisoning ability of the Pt/PANI-SnO$_2$/GC electrode may be explained as follows: PANI enwrapped on the surface SnO$_2$ is a good conductive matrix for dispersing Pt nanoparticles, which results in more active sites at the Pt/PANI-SnO$_2$ catalyst to oxidate the poisoning intermediates (CO$_{ads}$) to CO$_2$.

Conclusions

The PANI-SnO$_2$ composites, which were used to support Pt particles for methanol electro-oxidation, were prepared by chemical polymerization method in this paper. The electro-chemical properties of the Pt/PANI-SnO$_2$/GC electrode have been investigated by cyclic voltammetry, chronoamperom-etry, and chronopotentiometry in 0.5 M H$_2$SO$_4$ and 1.0 M CH$_3$OH aqueous solution. Comparing with the Pt/SnO$_2$/GC electrode, the Pt/PANI-SnO$_2$/GC electrode shows better electrochemical performance (larger ESA value, higher electrocatalytic activity and better anti-poisoning ability) under the same experimental conditions. These suggest that the Pt/PANI-SnO$_2$ catalysts will come into being a promising candidate for methanol oxidation in DMFC.
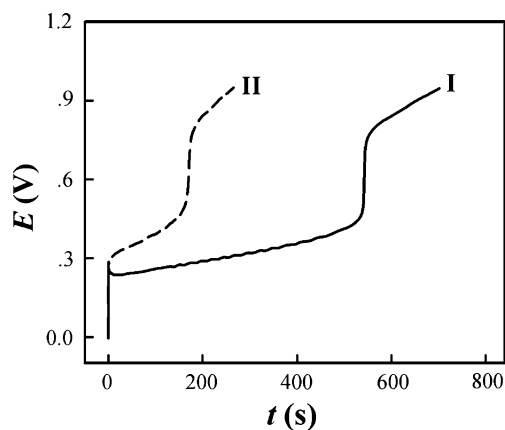

Fig. 8 Chronopotentiometric curves of the Pt/PANI-SnO$_2$/GC (curve *I*) and Pt/SnO$_2$/GC (curve *II*) electrodes in 0.5 M H$_2$SO$_4$+1.0 M CH$_3$OH aqueous solution. The value of the applied current is obtained at 0.5 V from the forward scan of the corresponding cyclic voltammogram. The loading mass of Pt, 8 μg

Fig. 7 Chronoamperograms of the Pt/PANI-SnO$_2$/GC (curve *I*) and Pt/SnO$_2$/GC (curve *II*) electrodes at 0.5 V in 0.5 M H$_2$SO$_4$+1.0 M CH$_3$OH aqueous solution. The loading mass of Pt, 8 μg

References

1. Antolini E, Salgado JRC, Gonzalez ER (2005) J Electroanal Chem 580:145
2. Lin YH, Cui XL, Yen C, Wai CM (2005) J Phys Chem B 109:14410
3. Wang JS, Xi JY, Bai YX, Shen Y, Sun J, Chen LQ, Zhu WT, Qiu XP (2007) J Power Sources 102:172
4. Paulus UA, Endruschat U, Feldmeyer GJ, Schmidt TJ, Bonnemann H, Behm RJ (2000) J Catal 195:383
5. Jayaraman S, Jaramillo TF, Baeck S-H, McFarland EW (2005) J Phys Chem B 109:22958
6. Shim J, Lee C, Lee H, Cairns EJ (2001) J Power Sources 102:172
7. Campos CL, Roldán C, Aponte M, Ishikawa Y, Carbrera CR (2005) J Electroanal Chem 581:206
8. Xu C, Shen PK (2004) Chem Commun 19:2238
9. Villullas HM, Mattos-Costa FI, Bulhŏes LOS (2004) J Phys Chem B 108:12898
10. Grass K, Lintz H-G (1997) J Catal 172:446
11. Gangal ND, Gupta NM, Iyer RM (1990) J Catal 126:13
12. Matsui T, Fujiwara K, Okanishi T, Kikuchi R, Takeguchi T, Eguchi K (2006) J Power Sources 155:152
13. Kawabe T, Tabata K, Suzuki E, Nagasawa Y (2001) Surf Sci 482–485:183
14. Santos AL, Profeti D, Olivi P (2005) Electrochim Acta 50:2615
15. Dimov N, Kugino S, Yoshio M (2003) Electrochim Acta 48:1579
16. Chen WX, Lee JY, Liu Z (2002) Electrochem Commun 4:260
17. Poizot P, Laruelle S, Grugeon S, Dupont L, Tarascon JM (2000) Nature 407:496
18. Lamy C, Leger J-M, Garnier F (1997) In: Nalwa HS (ed) Handbook of organic conductive molecules and polymer. Wiley, New York, p 471 3
19. Rajendra Prasad K, Munichandraiah N (2002) J Power Sources 103:300
20. Skothemin T, Elsenbaumer R (1998) Handbook of conductive polymers. Marcel Dekker, New York
21. Kim S, Park SJ (2008) Solid State Ion 178:1915
22. Dutta K, De SK (2007) Mater Lett 61:4967
23. Geng LN, Zhao YQ, Huang XL, Wang SR, Zhang SM, Wu SH (2007) Sens Actuators B 120:568
24. Hu ZA, Xie LY, Wang YX, Mo LP, Yang YY, Zhang ZY (2009) Mater Chem Phys 114:990
25. Pang HL, Lu JP, Chen JH, Huang CT, Liu B, Zhang XH (2009) Electrochim Acta 54:2610
26. Xia HS, Wang Q (2002) Chem Mater 14:2158
27. He YJ (2005) Mater Chem 43:2892
28. Geng LN, Zhao YQ, Huang XL, Wang SR, Zahng SM, Wu SH (2007) Sens Actuators B 120:568
29. Pozio A, Francesco MD, Cemmi A, Cardellini F, Giorgi L (2002) J Power Sources 105:13
30. Li WS, Lu J, Du JH, Lu DS, Chen HY, Li H, Wu YM (2005) Electrochem Commun 7:406
31. Xu C, Shen PK (2005) J Power Sources 142:27